

A comparison of four turbulence models with an application to the West Pacific Pool

AC. BENNIS¹, M. GOMEZ MARMOL², R. LEWANDOWSKI², T. CHACON ROBOLLO³, F. BROSSIER⁴

Abstract

In this study, we compare four turbulence models which are used for the parametrization of the oceanic boundary layer. Two of these models, called R 224 and R 22, are new and the others are Paganowski and Philander's model (R 213 model) and Gent's model (R 23 model). These four models depend on the bulk Richardson number, which is coherent with the studied region, the West Pacific Pool, because of the large mean shear associated with the equatorial undercurrent. For the numerical implementation, we use a non-conservative numerical scheme. We compare these four models on three criteria : the surface current intensity, the thermocline's form and the mixed layer depth. We take an interest in a linear case and in a realistic case from the TOGA-TAO array. In the both cases, the R 213, R 23 and R 224 models show a mixed layer depth dependency due to the wind stress intensity. The computed mixed layer depth is the same for these three models. The R 213 and R 224 models give similar results for the surface current intensity. In the linear case, the R 224 model products a sharpest thermocline in comparison to R 213 model. In the realistic case, R 23, R 213 and R 224 model simulate a similar thermocline. In the case of a density gradient inversion on the initial profile, only the R 224 model gives a realistic result. In addition, we studied the equilibrium solution and we note that it is a linear solution which is in agreement with Bennis and al [1]. To conclude, the R 224 model has, on the whole, the same behavior as the Paganowski and Philander's model, moreover it can be used in more situations.

Summary 0.1 **Keywords** : vertical mixing, Richardson number, mixing layer, equilibrium, stability.

1 Introduction

The presence of an homogeneous layer near the surface of the ocean has been observed since a long time. The so called "mixed layer" presents almost constant profiles of temperature and

¹ IRMAR, Université de Rennes 1, Campus de Beaulieu, 35042 Rennes Cedex, France

² Departamento de Ecuaciones Diferenciales y Análisis Numérico, Universidad de Sevilla. C/Tarifa, s/n. 41080, Sevilla, Spain

³ IRMAR, Université de Rennes 1, Campus de Beaulieu, 35042 Rennes Cedex, France

⁴ Departamento de Ecuaciones Diferenciales y Análisis Numérico, Universidad de Sevilla. C/Tarifa, s/n. 41080, Sevilla, Spain

⁴ IRMAR, Université de Rennes 1, Campus de Beaulieu, 35042 Rennes Cedex, France

salinity. The bottom of the mixed layer corresponds either to the top of the thermocline, zone of large gradients of temperature, or to the top of the zone where haline stratification is observed [38]. Some attempts to describe this phenomenon can be found for example in Dufant [5], Rossby-Montgomery [34] and Lewandowski [21]. The effect of the wind-stress acting on the sea-surface was then considered to be the main forcing of this boundary layer. Observations in situ were completed by laboratory experiments [4] and more recently by numerical modelizations of the mixed layer. An historical of these different approaches can be found in Käse [14]. Käse quoted the model of Kraus and Turner [15] as the first applied mixed layer model. According to observations, the thickness of the mixed layer can vary between ten meters and a few hundred of meters, depending on the latitude. The mixed layer presents also important seasonal variations. Mixing processes are intense in the homogeneous boundary layer, much weaker near the thermocline or in the deep ocean. The effects of local fluxes of heat and momentum across the sea-surface induce turbulence and then mixing processes in the surface layer. The dynamical response of the ocean, and especially small scale turbulence, has a significant effect on mixing processes. This is true particularly in tropical areas. The rate of kinetic energy dissipation and the vertical turbulent fluxes of heat and mass cannot be measured directly, but they can be deduced from measurements of vertical temperature gradients and horizontal velocity [33]. Such experiments showed that turbulent dissipation is higher near the equator than in low latitudes [10], [11], [7]. Therefore in order to modelize the mixed boundary layer and to represent correctly the mixing processes, it is necessary to define a parametrization of turbulent diffusion. The mixed layer being strongly dominated by vertical fluxes, attention is focused on vertical mixing which requires a closure model in order to represent the Reynolds stress. Recently, Gousse et al. [9] studied the sensitivity of a global model to different parametrizations of vertical mixing. They insist on the crucial role of mixing in the upper oceanic layers : it has a direct impact on the sea surface temperature and then on ice evolution, but affects also the vertical profile of velocity by redistributing the momentum [2].

Classically, mixing parametrizations consist in the definition of turbulent eddy viscosity and diffusivity coefficients. These coefficients can be chosen either as constants or as fixed profiles [13]. This is a simple but crude parametrization since variations of mixing with time and location are forbidden. A more suitable method is to define these coefficients as functions of processes governing the mixing. In tropical oceans vertical stratification and velocity shear are natural parameters since, following Philander [33] one of the reasons for higher turbulent dissipation near the equator than in low latitudes is the large vertical shear observed in tropical currents. Paganowski and Philander [30] proposed a formulation for eddy viscosity and diffusivity coefficients depending on the Richardson number which represents the ratio between buoyancy effects and vertical shear. The Richardson number dependent formulations allow strong mixing in high shear regions with low stratification, and low mixing elsewhere. It has to be noted that stratification tends to reduce turbulence and therefore mixing processes. More recently, parametrizations based on sophisticated turbulence closure schemes have been developed. These models can be classified in two groups. One kind of methods defines eddy viscosity and diffusivity

coefficients as functions of the turbulent kinetic energy (TKE) : This method, used by Blanke and Deleuze [2] of course requires a closed equation in order to compute the TKE. The second group uses the "K profile parametrization" (KPP) : These methods are based on the Monin-Obukhov theory and use similarity scalings in the near surface layers. Large et al. have developed such models [18], [16], [17].

In this paper we do not study such sophisticated models but we focus our attention on the behaviour of the Richardson number depending models: the basic one proposed by Paganowski-Philander and three variants used in [8], [21], [9]. The Richardson number can be considered as a characteristic number in the cases of forced convection or static stability. In the case of free convection, the flow is essentially driven by buoyancy and the Richardson number is no more representative of the physics of the flow. Therefore it seems reasonable to restrict the domain of validity of the Richardson number depending models to the cases of forced convection or static stability, these models being replaced by convective adjustment in the case of free convection. For each of the studied models, we discuss hereafter the existence of equilibrium solutions and study their stability. We consider surface fluxes including wind-stress but also surface heating or cooling, precipitations or evaporation. Therefore the density in the upper layer can increase and give rise to inverted profiles of density.

We prove in section 2.2 that it exists equilibrium solutions characterized by linear profiles of velocity and density, therefore the equilibrium states of the studied models do not correspond to mixed homogeneous layers. For some positive density fluxes at the surface, it can exist two or three equilibrium profiles depending on the model we use. Equilibrium solutions of these models are reached after all transient effects of turbulence have been adjusted by the flow. Therefore, equilibrium solutions must be stable, in the sense that small perturbations imposed at some time t_0 must be damped for $t > t_0$.

We study the stability of equilibrium profiles in section 2.3 through a linear approach ("linear stability"). We give simple stability conditions which are illustrated for the different Richardson number depending models studied in this paper. Whatever the parametrization of the eddy coefficients, the linear equilibrium profiles corresponding to a Richardson number $R > 0$ are all stable. It exists an interval $[R_1; R_2]$ with $R_1 < R_2 < 0$ such that for $R \in [R_1; R_2]$ the equilibrium profiles are unstable and therefore the validity of the modelization can be questioned. Of course the values of the bounds R_1 and R_2 are different for each model and, depending on the formulation, the interval $[R_1; R_2]$ may be located inside or outside the domain of validity of the model.

Section 3 is devoted to numerical experiments. The stability or instability of equilibrium profiles is illustrated for different surface fluxes and for the different parametrizations. Then we have studied the behaviour of the different models when the initial velocity field is more realistic, for example when profiles characteristic of the tropical areas are imposed at initial time. The purpose of these mixing models, based on the Richardson number, is to produce a mixing layer; then this homogeneous surface layer must be evidenced in the numerical results. We will see in section 3 that only one among the studied models satisfies this requirement.

2 Modelization of the mixing layer

2.1 Setting of the problem

Variables used in this paper for the description of the mixing layer are statistical means of the horizontal velocity and of the density denoted by $(u; v; \rho)$: In ocean, the density is function of temperature and salinity through a state equation. So, we consider the density as an idealized thermodynamical variable which is intended to represent temperature and salinity variations. The formation of the mixing layer is a response to air-sea interactions: wind-stress, solar heating, precipitations or evaporation acting on the sea surface. The variability of temperature is considered as essential to understand the response of the ocean. For example the existence of a sharp thermocline is a well known feature of the tropical areas. The thermal inertia of the water column is linked with the depth of the thermocline, which then influences the sea-surface temperature. The role of the haline stratification, sometimes considered as less important, has been recently evidenced by Vialard and Delecluse [38]: a numerical modelization of the tropical Pacific produces a "barrier layer" depending on surface forcings and large scale circulation. The term "barrier layer" refers to the water column located between the bottom of the mixed layer and the top of the thermocline. It is present when the isohaline layer is shallower than the isothermal layer and then the depth of the mixed layer is controlled by the salinity.

The model studied hereafter is not expected to describe all the phenomena occurring in the mixing layer. Its purpose is only a better understanding of a classical closure model. Therefore we shall use simplified equations governing the variables u, v and ρ , the density being considered as a global thermodynamical variable representing both temperature and salinity variations.

The mixing layer being strongly dominated by vertical fluxes, we shall suppose that u, v and ρ are horizontally homogeneous and we so obtain a one-dimensional modelization. The Coriolis force will be neglected, which is valid in tropical oceans. Then the equations governing the mixing layer are

$$\begin{aligned} \frac{\partial u}{\partial t} &= \frac{\partial}{\partial z} h u^0 w^0 i; \\ \frac{\partial v}{\partial t} &= \frac{\partial}{\partial z} h v^0 w^0 i; \\ \vdots \frac{\partial}{\partial t} &= \frac{\partial}{\partial z} h^0 w^0 i; \end{aligned} \quad (1)$$

where u^0, v^0, w^0 represent the fluctuations of horizontal velocity, vertical velocity and density. The notation h^0 signifies that the quantity is statistically averaged. Equations (1) are classical equations corresponding to a modelization of a water column. Such equations can be found in [19] as the equations of the boundary layer. Equations (1) are not closed and then the vertical fluxes appearing in the right-hand side have to be modeled. We study in this paper the behaviour of a very classical closure modelization that uses the concept of eddy coefficients

in order to represent turbulent fluxes. So we set

$$\begin{aligned} u^0 w^0 &= 1 \frac{\partial u}{\partial z}; \\ v^0 w^0 &= 1 \frac{\partial v}{\partial z}; \\ w^0 &= 2 \frac{\partial}{\partial z}; \end{aligned}$$

Coefficients α_1 and α_2 are called vertical eddy viscosity and diffusivity coefficients and will be expressed as functions of the Richardson number R defined as

$$R = \frac{g}{\rho_0} \frac{\frac{\partial}{\partial z}}{\left(\frac{\partial u}{\partial z} \right)^2 + \left(\frac{\partial v}{\partial z} \right)^2};$$

where g is the gravitational acceleration and ρ_0 a reference density (for example $\rho_0 = 1025 \text{ kg m}^{-3}$). The set of equations, initial and boundary conditions governing the mixing layer can now be written

$$\begin{aligned} \frac{\partial u}{\partial t} + \frac{\partial}{\partial z} \left(1 \frac{\partial u}{\partial z} \right) &= 0; \\ \frac{\partial v}{\partial t} + \frac{\partial}{\partial z} \left(1 \frac{\partial v}{\partial z} \right) &= 0; \\ \frac{\partial}{\partial t} \left(2 \frac{\partial}{\partial z} \right) + 2 \frac{\partial}{\partial z} &= 0; \quad \text{for } t > 0 \text{ and } h \leq z \leq 0; \\ u = u_b; v = v_b; &= b \quad \text{at the depth } z = h; \\ 1 \frac{\partial u}{\partial z} = - \frac{a}{\rho_0} V_x; \quad 1 \frac{\partial v}{\partial z} = - \frac{a}{\rho_0} V_y; \quad 2 \frac{\partial}{\partial z} &= Q \quad \text{at the surface } z = 0; \\ u = u_0; v = v_0; &= 0 \quad \text{at initial time } t = 0; \end{aligned} \tag{2}$$

In system (2), the constant h denotes the thickness of the studied layer that must contain the mixing layer. Therefore the circulation for $z < h$, under the boundary layer, is supposed to be known, either by observations or by a deep circulation numerical model. This justifies the choice of Dirichlet boundary conditions at $z = h$, u_b , v_b and b being the values of horizontal velocity and density in the layer located below the mixed layer. The air-sea interactions are represented by the fluxes at the sea-surface : V_x and V_y are respectively the forcing exerted by the zonal wind-stress and the meridional wind-stress and Q represents the thermodynamical fluxes, heating or cooling, precipitations or evaporation. We have $V_x = C_D u_a^2 f$ and $V_y = C_D v_a^2 f$, where $u_a^2 = (u_a; v_a)$ is the air velocity and C_D a friction coefficient.

We study hereafter four different formulations for the eddy coefficients $\alpha_1 = f_1(R)$ and $\alpha_2 = f_2(R)$: Functions f_1 and f_2 can be defined as

$$f_1(R) = \alpha_1 + \frac{1}{(1+5R)^2}; \quad f_2(R) = \alpha_2 + \frac{f_1(R)}{1+5R} = \alpha_2 + \frac{1}{1+5R} + \frac{1}{(1+5R)^3}; \quad (3)$$

Formulation (3) corresponds to the modeling of the vertical mixing proposed by Pacanowski and Philander [30]. They proposed for coefficients α_1 and α_2 the following values: $\alpha_1 = 1 \cdot 10^{-4}$; $\alpha_1 = 1 \cdot 10^{-2}$; $\alpha_2 = 1 \cdot 10^{-5}$ (units: $\text{m}^2 \text{s}^{-1}$). This formulation has been used in the OPA code developed in Paris 6 University [2], [23] with coefficients $\alpha_1 = 1 \cdot 10^{-6}$; $\alpha_1 = 1 \cdot 10^{-2}$; $\alpha_2 = 1 \cdot 10^{-7}$ units: $\text{m}^2 \text{s}^{-1}$. The selection criterion for the coefficients appearing in these formulas was the best agreement of numerical results with observations carried out in different tropical areas. A variant of formulation (3), proposed by Gent [8], is

$$f_1(R) = \alpha_1 + \frac{1}{(1+10R)^2}; \quad f_2(R) = \alpha_2 + \frac{2}{(1+10R)^3} \quad (4)$$

with $\alpha_1 = 1 \cdot 10^{-4}$; $\alpha_1 = 1 \cdot 10^{-1}$; $\alpha_2 = 1 \cdot 10^{-5}$; $\alpha_2 = 1 \cdot 10^{-1}$ (units: $\text{m}^2 \text{s}^{-1}$): A formulation similar to (4) when replacing $10R$ by $5R$ and varying the values of the coefficients α_1 ; α_2 between the surface and the depth 50m is used in [9].

In this paper, we will also study the properties of two other formulations close to formula (3):

$$f_1(R) = \alpha_1 + \frac{1}{(1+5R)^2}; \quad f_2(R) = \alpha_2 + \frac{f_1(R)}{(1+5R)^2} = \alpha_2 + \frac{1}{(1+5R)^2} + \frac{1}{(1+5R)^4}; \quad (5)$$

and

$$f_1(R) = \alpha_1 + \frac{1}{(1+5R)^2}; \quad f_2(R) = \alpha_2 + \frac{2}{(1+5R)^2}; \quad (6)$$

with $\alpha_1 = 1 \cdot 10^{-4}$; $\alpha_1 = 1 \cdot 10^{-2}$; $\alpha_2 = 1 \cdot 10^{-5}$; $\alpha_2 = 1 \cdot 10^{-3}$ units: $\text{m}^2 \text{s}^{-1}$:

Eddy viscosity α_1 defined by (5) or (6) is the same as the coefficient given by Pacanowski and Philander. The definition of the eddy diffusivity coefficient α_2 differs by the exponent of the term $(1+5R)$. Formula (6) is a simplified version of (5) where α_2 can be considered as a mean value of $\alpha_2 = f_2(R)$:

In formulas (3) to (6), the eddy coefficients α_1 and α_2 are defined as functions of the Richardson number R through the terms $(1+R)^n$ appearing at the denominator. Hereafter, these four formulations will be denoted respectively by R-2-13, R-2-3, R-2-24 and R-2-2 where R signifies Richardson number and the integer values are the exponents of $(1+R)$ in the definitions of α_1 and α_2 :

Eddy coefficients defined by relations (3) to (6) present all a singularity for a negative value of the Richardson number $R = 0.2$ or $R = 0.1$: We have plotted in Figure 1 the curves $\alpha_1 = f_1(R)$. In formulations (3) or (4) the coefficient of eddy diffusivity α_2 becomes negative for values of R lower than 0.2 or 0.1, and therefore the model is no more valid. The curves $\alpha_2 = f_2(R)$ obtained with formulations (3), (5) and (6) are plotted in Figure 1, for $R > -0.2$.

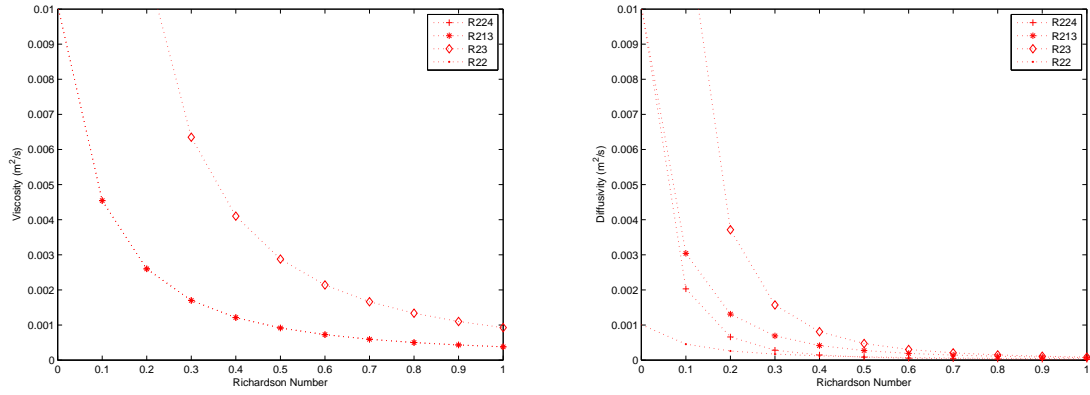


Figure 1 : Viscosity ($f_1(R)$) for all models (left hand side) and diffusivity ($f_2(R)$) for all models (right hand side)

Problem (2) coupled with one of the definitions (3) to (6) for eddy coefficients retains the vertical shear and buoyancy effect which are two important processes for the generation of the mixed boundary layer, especially in tropical areas.

3 Numerical Simulation

In this section, we study a water column which is thousand meters deep. We compare the four turbulence model on several points. We interest to the mixed layer depth, the form of thermocline and the intensity to the surface current. It's more difficult to determine is the mixed layer depth. The mixed layer represent a range which surface fluxes have been mixed in the recent past. We distinguish this layer to the mixing layer which is actively being mixed by the action of surface fluxes. This distinction has been observed notably in observations by Shay et al [35]. The mixed layer depth has been studied notably by Levitus [20], Rainier and Gregg [3], Montrey and Levitus [27], De Boyet Montegut [26]. There is two type of criterion for the determination of mixed layer depth. The first is based on the density difference with the surface density and the second is based on gradient density difference. In this work, we use a criterion based on the density difference equal to 0.01 kg m^{-3} . This criterion is standard for equatorial region and it is used notably by Peters and al [32].

First, we study the time evolution of linear initial profile and equilibrium solution. We compare the performance of different turbulence model. The case of linear initial profile was treated notably by Tabak and al [37]. In second, we interest to a realistic case and we study an equatorial Pacific region. In the past, for this case, the comparison of different turbulence model including the PP was done by notably Li and al [22], Halpern and al [12] and Smith and al [36]. Li and al compare the PP model and the KPP model of Large and Gent [17]. Halpern and al and Smith and al study the PP model and the MY model of Mellor and Yamada [25]. In the next paragraph, we give more details on the studied region and we perform how the new model represent the oceanic mixed layer.

This work was done with matlab code. Our numerical scheme use finite differencing in non-conservative form. It is described in the section below. Traditionally, the conservative form is used as in the work of Tabak and al [37].

3.1 Finite Difference Scheme

In this part, we construct a finite difference scheme to solve the equations (7) numerically.

$$\begin{aligned}
 & \frac{\partial u}{\partial t} + \frac{\partial}{\partial z} \left[\frac{\partial u}{\partial z} \right] = 0; \\
 & \frac{\partial v}{\partial t} + \frac{\partial}{\partial z} \left[\frac{\partial v}{\partial z} \right] = 0; \\
 & \frac{\partial}{\partial t} \left[\frac{\partial}{\partial z} \left[\frac{\partial}{\partial z} \right] \right] = 0; \text{ for } t > 0 \text{ and } h \leq z \leq 0;
 \end{aligned} \tag{7}$$

We replace the continuous variables by discrete variable such as $t = n \Delta t$ with $n = 1, 2, \dots, N$ and $z = (i - N/2)h$ with $i = 1, 2, \dots, N$. We have discretized the 1D domain in z -levels where z is the vertical coordinate. The non-conservative finite-difference form of equation (7) can be written as :

$$\begin{aligned}
& \frac{u_i^{n+1} - u_i^n}{t} - \frac{1)_{i-1}^n - 1)_{i+1}^n}{z} + \frac{u_i^{n+1} - u_{i-1}^{n+1}}{z} \frac{!}{1)_{i-1}^n} - \frac{u_{i+1}^{n+1} - 2u_i^{n+1} + u_{i-1}^{n+1}}{z^2} \frac{!}{= 0;} \\
& \frac{v_i^{n+1} - v_i^n}{t} - \frac{1)_{i-1}^n - 1)_{i+1}^n}{z} + \frac{v_i^{n+1} - v_{i-1}^{n+1}}{z} \frac{!}{1)_{i-1}^n} - \frac{v_{i+1}^{n+1} - 2v_i^{n+1} + v_{i-1}^{n+1}}{z^2} \frac{!}{= 0;} \\
& \frac{n+1}{t} \frac{n}{z} - \frac{2)_{i-1}^n - 2)_{i+1}^n}{z} + \frac{n+1}{z} \frac{n+1}{z} \frac{!}{2)_{i-1}^n} - \frac{n+1}{z^2} \frac{2}{z} \frac{n+1}{z} \frac{n+1}{z} \frac{!}{= 0;}
\end{aligned} \tag{8}$$

We use a second-order central difference scheme for the second space derivative and a first-order backward difference scheme for the first space derivative. In time, we use a semi-implicit scheme with an explicit viscosity, diffusivity and an implicit velocity, density. These previous scheme can be written as :

$$\begin{aligned}
\text{Second-order central difference scheme : } \frac{\partial^2 u}{\partial z^2} \Big|_i^{n+1} &= \frac{u_{i+1}^{n+1} - 2u_i^{n+1} + u_{i-1}^{n+1}}{z^2} \\
\text{First-order backward difference scheme : } \frac{\partial u}{\partial z} \Big|_i^{n+1} &= \frac{u_i^{n+1} - u_{i-1}^{n+1}}{z}
\end{aligned}$$

In this study, we choose a uniform grid spacing, z , equal to 5 m and a time step, t , equal to 60 s with a basin size to 100 m to maximize resolution while preserving computational efficiency. The boundary conditions are treated with a first-order backward difference scheme and therefore, for 8, we have a one order difference finite scheme. The initial conditions are implemented from the initial Richardson number calculated from the velocity and density initial profile.

3.2 Linear case

In this section, we study in the first part, the time evolution of a linear solution and in the second part, the equilibrium solution of the equation 7.

3.2.1 Time evolution of the linear initial profile

In this section, we perform the time evolution of the initial linear profile. We compare the four turbulence model and we take an interest in the intensity of the surface current, in the thermocline's form and in the depth of mixed layer. This type of initial profile was studied notably by Tabak and al [37] and Deleersnijder [6]. We investigate two case, a shallow wind and a strong wind at the surface. We have the same buoyancy flux for all case equal to $1 \cdot 10^{-6} \text{ kg} \cdot \text{s}^{-1} \text{ m}^{-2}$.

First case : A shallow wind at the surface We take the zonal wind at the surface equal to 3 m s^{-1} and the meridional wind equal to 0.4 m s^{-1} . The initial profile are linear and are

showed on the figure 2. We have not a mixed layer and the velocity profile does not represent the reality. This study aims to perform the wind stress impact and to validate our modelization.

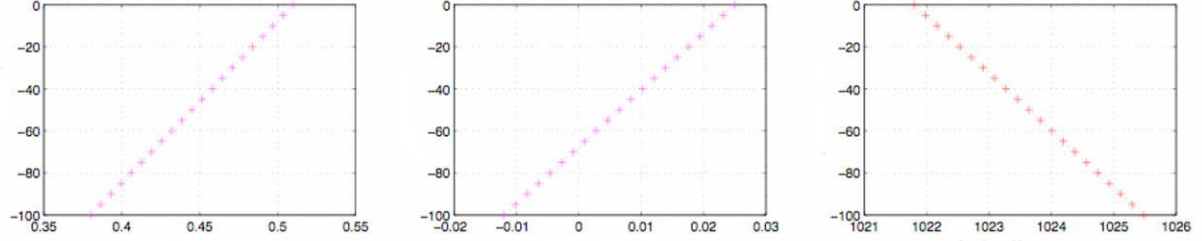
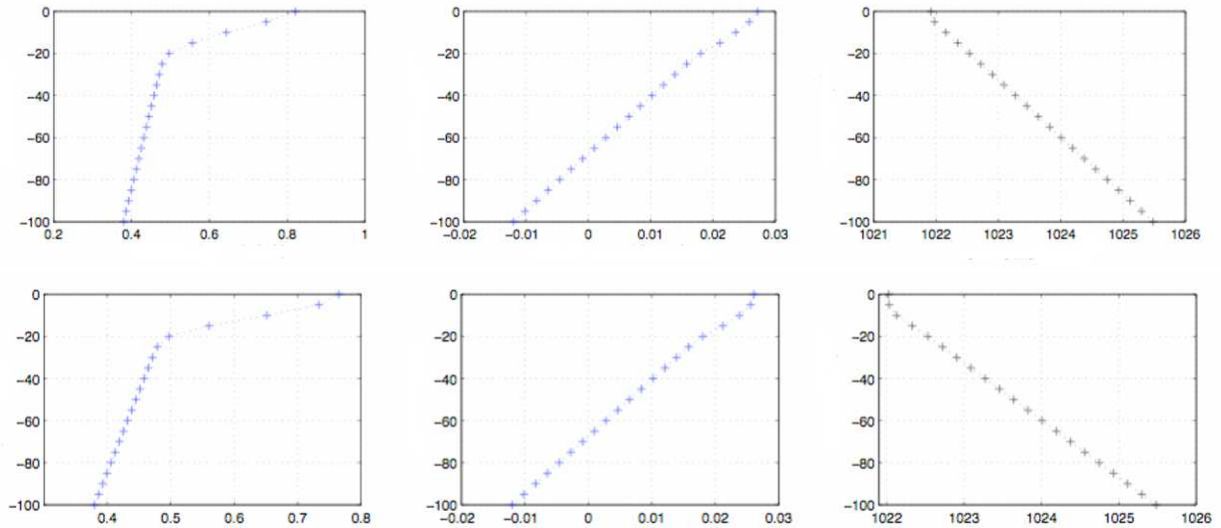


Figure 2 : Initial zonal velocity, meridional velocity and density profile.

The results of numerical simulation are shown on the figure 3. The simulate time is 48 h. We have a similar comportment for all turbulence models. For the density, we observe no mixed layer for all model. However, there is a zone of constant density in the first 20 meters for R213, R23, R22 models. This zone is less intense for R224 model. For the R213 model, the surface density is more high than for the others. The flow from the twenty meters is similar to the initial flow because of the shallow forcing at the surface. For the surface current, the R213 and R23 model gives a same results, the form and the value are very similar. The R22 model show a surface current which is lightly different in the first 20 meters compared with this of R213 and R23 models. However, the value at the surface is the same. We apply an eastward wind at the surface therefore it is coherent that we have a zonal surface current larger than in initial configuration. In the same order, we apply a northward wind at the surface but its intensity is too weak and therefore we have few difference with the initial configuration. However, we note a increasing in its intensity, that is agree with the applied forcing at the surface.



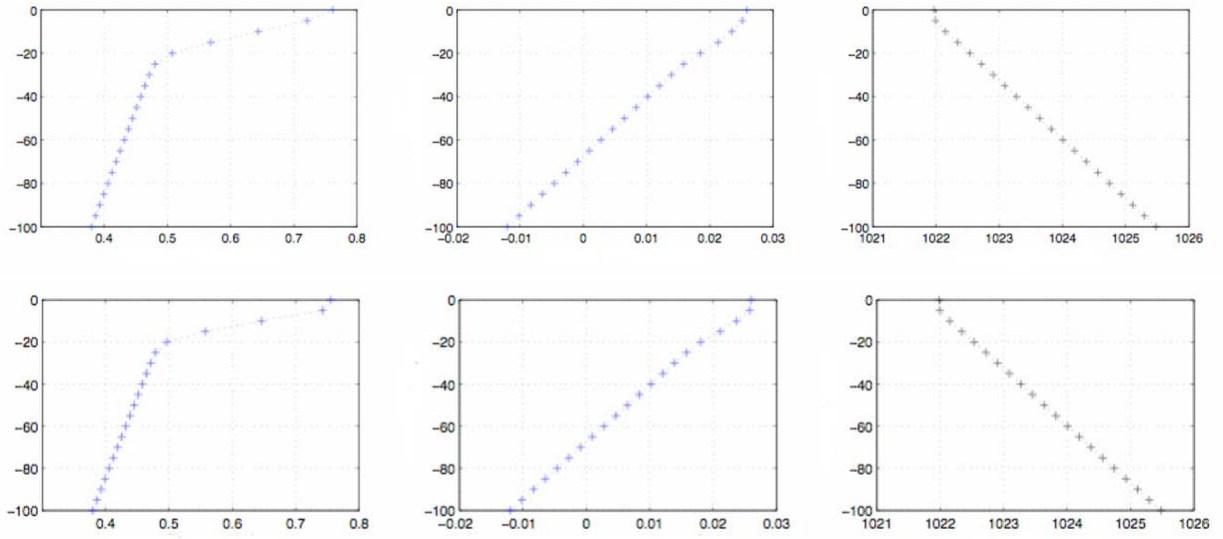
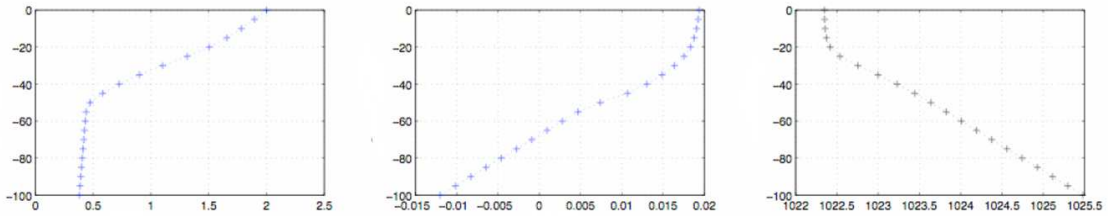


Figure 3 : Final zonal velocity, meridional velocity and density profile for respectively from top to below for R 224, R 213, R 23 and R 22 model.

Second case : A strong wind at the surface We was done a numerical simulation for a strong wind stress at the surface. We simulate a time equal to 48 h. We take a zonal wind equal to 11.7 m s^{-1} and a meridional wind equal to 0.4 m s^{-1} . We keep a surface buoyancy flux equal to $1 \cdot 10^{-6} \text{ kg s}^{-1} \text{ m}^{-2}$. The results are shown on the figure 4. We observe for three case, on the density profile, the formation of mixed layer. According to the same criterion that Peters et al [32], we have a mixed layer depth ten meter deep for R 224, R 23, R 213 model. The R 22 model does not produce a mixed layer. It present, as the shallow wind case, a zone of constant density five meter deep. For the surface current, we observe similar results for the R 213 and R 224 models. The R 213 model underestimate this current whereas R 22 overestimate it in comparison with R 213 and R 224 models. The thermocline simulated by the R 224 model is sharpest than for R 213 model. The results obtained with the four models are not very different in the lower layer (60-100m) because the surface fluxes do not affect the deep water column.



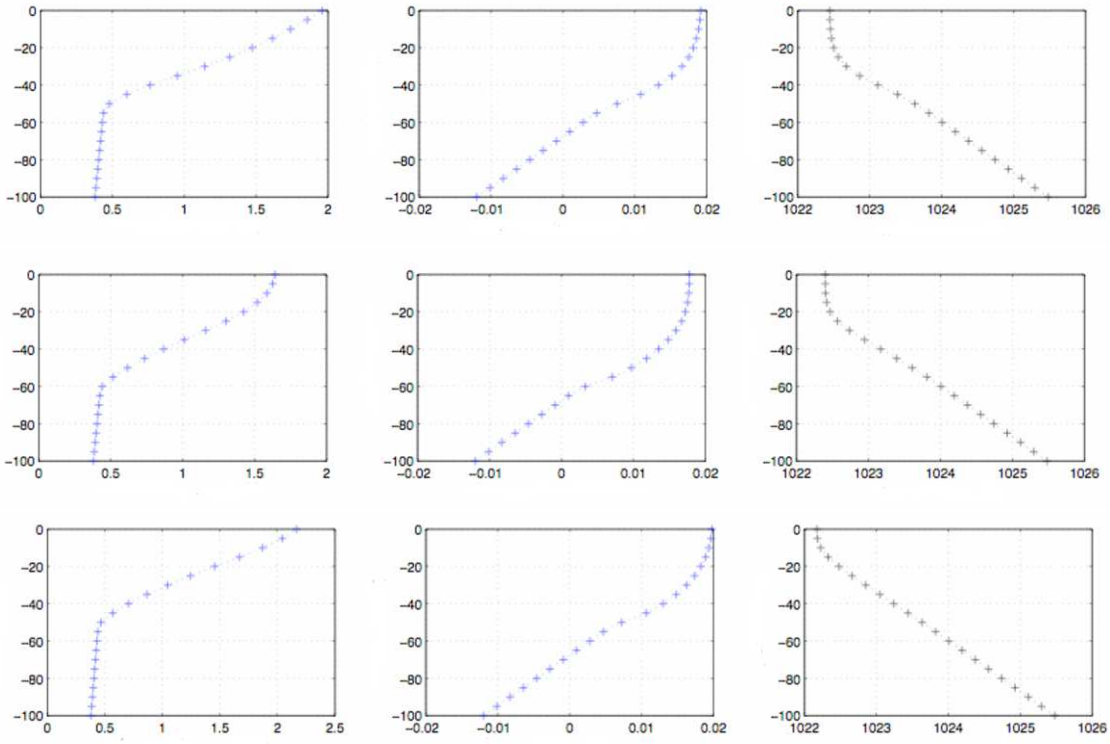


Figure 4 : Final zonal velocity, meridional velocity and density profile for respectively from top to below for R 224, R 213, R 23 and R 22 model.

3.2.2 Equilibrium solution

In this paragraph, we take an interest to the equilibrium solution. For this, we simulate a long time corresponding to 10000h. We take a initial profile which is not linear and represent the mean state of the equatorial Pacific Ocean at 165°E, 0°N for the date of 17/06/91. These data come from the Tropical Atmosphere Ocean (TAO) array (McPhaden [24]) which is explained in details in paragraph 3.4.1. The initial zonal velocity profile show several eastward current which have a maximum located at the surface and to 70 m and several westward current which have a maximum located to 45 m and 90 m. In the same order, the initial meridional velocity profile show a southward current and two northward current. On the initial density profile, we observe a mixed layer thirty five meter deep.

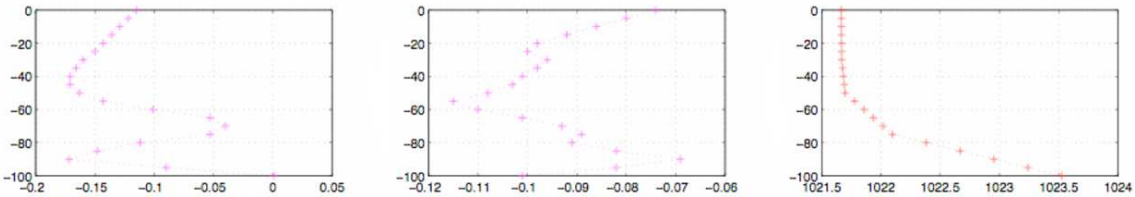


Figure 5 : The initial profile of zonal velocity, meridional velocity, in-situ density.

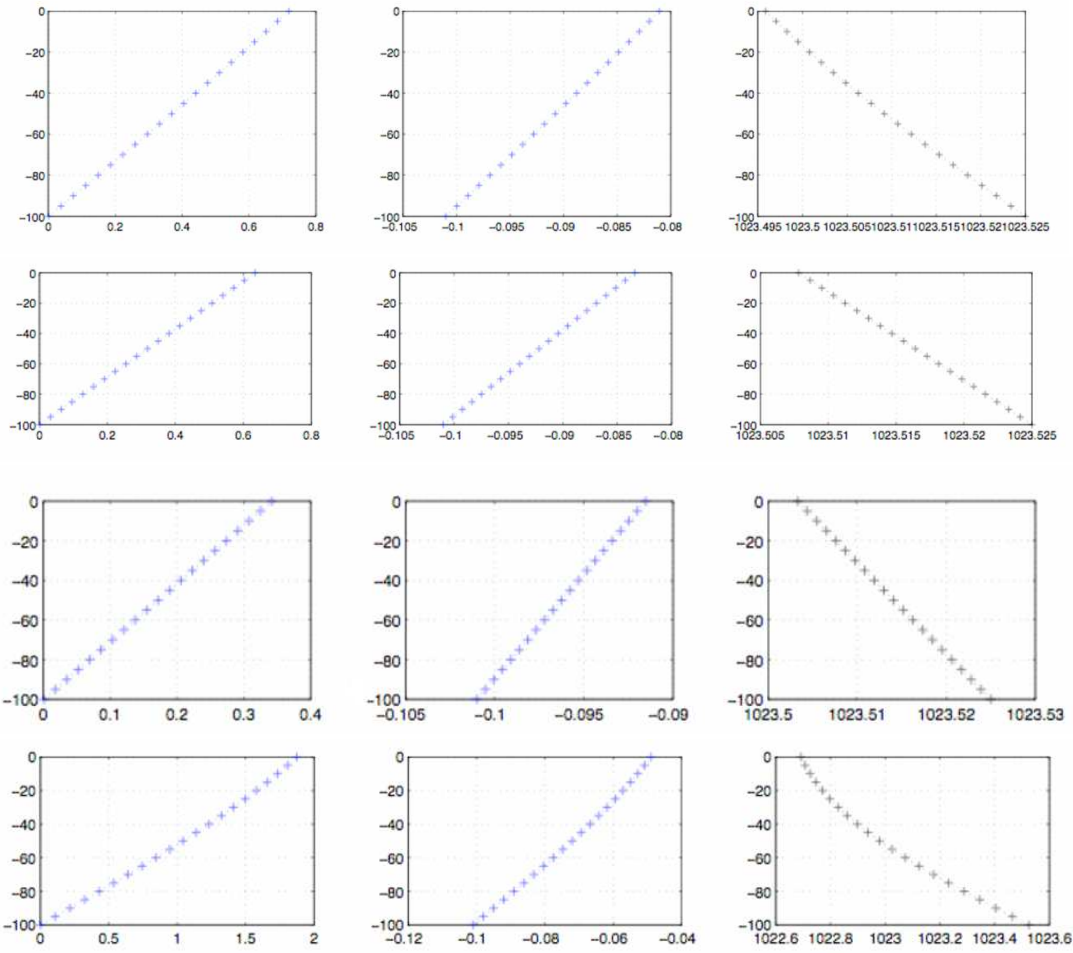


Figure 6 : Zonal velocity, meridional velocity and density for respectively, from top to bottom , R 224, R 213, R 23, R 22 model

On the figure 6, we observe that the four turbulence model gives a linear profile for the simulated time. However, the results of R 22 model are inferior to the ones of the others models. The R 213 and R 224 gives a same order surface current. The R 23 model underestimates this current while the R 22 model overestimates it. This fact corroborate the existence of a linear equilibrium solution obtained by Bennis and al [1].

3.3 Summary on the linear case

In the first, we explain the advantage and drawback of the R 213 model. Peters and al [31] have shown by comparison with experiment that the PP scheme underestimates the turbulent mixing at low R_i , while overestimating the turbulence mixing at high R_i . This scheme simulate a thermocline which is much too diused in comparison with the observations. In addition, the PP scheme overestimates the surface current [12],[28].

In second, we discuss on the advantage and drawback of the R 23 model. This model gives realistic results in the West Pacific Warm Pool. It simulate a sharp thermocline which is coherent with

the observation [8]. In opposition, it is not good for the eastern pacific because the thermocline is more diffuse than in reality. This model gives a good results for the annual average SST (Sea Surface Temperature) at the equator.

The results of linear case show that :

For the evolution of the linear initial profile, we observe that the wind stress intensity is fundamental. In fact, according to this intensity, we have a mixed layer or not. In the first case, where we have a shallow wind at the surface, there is no mixed layer and in the second case, where we have a strong wind at the surface, there is a mixed layer.

The analysis of the figure 7 clarify several points. For the surface current, R 224 and R 213 gives similar results. These models have the same problem that is to overestimate this current. R 22 represent a strong surface current that is not agree with the observations. The density profile show that R 224, R 23, R 213 simulate a mixed layer that is the same depth. The R 224 simulate a sharpest thermocline than the R 213 model, that is good. In fact, one of drawback of R 213, is that the thermocline simulated is too much diffuse in comparison with the observation. The R 22 model does not represent a mixed layer. This model is not good for the simulation of the surface current and the mixed layer.

For the study of the equilibrium solution, the numerical results show the existence of a linear solution for the equilibrium state. This is agree with the work was done by [1].

3.4 Realistic case

In this section, we study, in particular, a equatorial Pacific region call the West-Pacific Warm Pool, located at the equator between 120°E and 180°W. It is a zone where the sea temperature is high and quasi-constant along the year (28–30°C). These water are little salinated because of strong precipitation. We perform the evolution in time of velocity and density profiles driven by constant surface fluxes, and starting from given initial conditions. The purpose of this numerical experiment is to compare the behaviour of the four studied models. First, we comment the initial data since we expose the numerical results.

3.4.1 The initial data

In this work, we use data available from the Tropical Atmosphere Ocean (TAO) array (McPhaden [24]). This project aims to study the exchange between the tropical oceans and the atmosphere. These data have been very used for numerical simulation. For our research, we use the velocity data from the ACDP (Acoustic Doppler Current Profiler) measurements and the potential density data. We was done as hypothesis that for our depths the potential density was equal to the density in-situ. In fact, the depths are weak and in consequence the pressure effects are negligible. For obtain the adequate profile for the spacing grid, we have interpolated the data by an one-order linear interpolation. Our study was done in 0°N; 165°E. Since with these profile, we initialize the matlab code et we obtain the results commented below.

3.4.2 Numerical Results

Sensitivity to the wind stress We show, in the previous section, that the flow was sensible to the wind stress intensity. In this paragraph, we perform if this is the same comportment is observed with realistic data. For the numerical simulation, we take a buoyancy flux equal to $1:10^{-6} \text{ kg m}^{-2} \text{ s}^{-1}$ which correspond to heat flux equal, in absolute value, to 11 W m^{-2} . This heat flux is agree to the study of Gent [8] which show that between 140°E 180°E and 10°N 10°S , the heat flux vary between 0 W m^{-2} and 20 W m^{-2} . In the next, we take the same heat flux. In the first part, we take an interest in a shallow wind at the surface, with a zonal component equal to $2:1 \text{ m s}^{-1}$ and a meridional component equal to $1:0 \text{ m s}^{-1}$. This values of wind stress are realistic with the studied region and the time period. We study an interval some 15 days time, between the 15/06/91 and the 15/07/91. The second case is less realistic since the wind stress was taken stronger the reality. However, these values have a physical sense since they are characteristic of another period in studied year. We take a zonal wind equal to $8:1 \text{ m s}^{-1}$ and a meridional wind equal to $2:1 \text{ m s}^{-1}$ for this second case.

The initial profile are plotted on the figure 7. The initial zonal velocity profile presents a westward current in the surface layer and, below it, a strong eastward undercurrent whose maximum is located about 55 m . Deep, we observe a westward undercurrent. The initial density profile show no mixed layer according to the same criterion that Peters and al [32] to determine this depth.

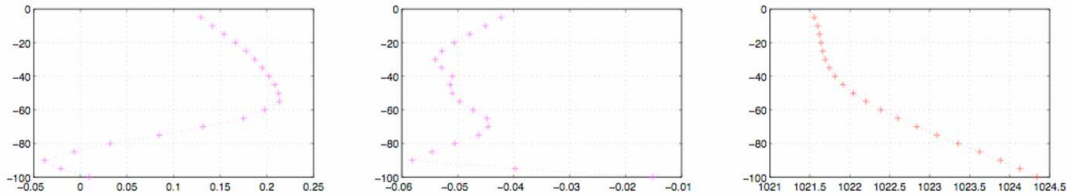
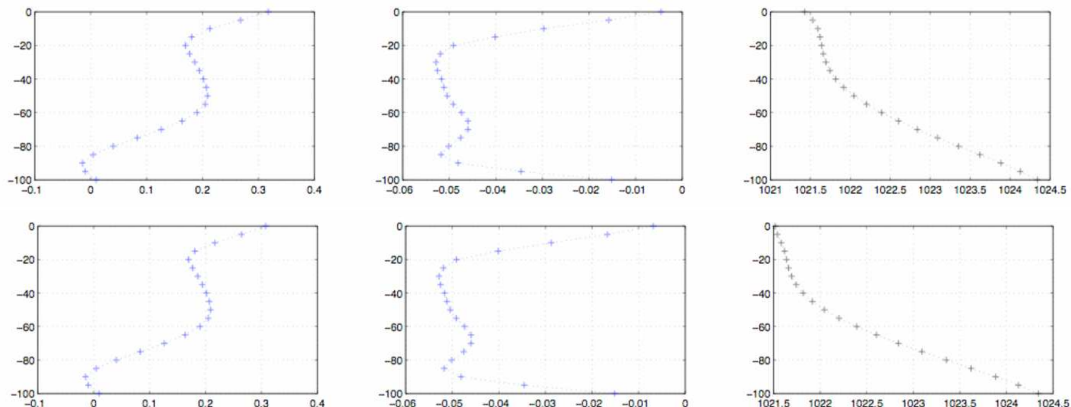


Figure 7 : Initial zonal velocity, meridional velocity and density profile

First Case : Shallow wind at the surface



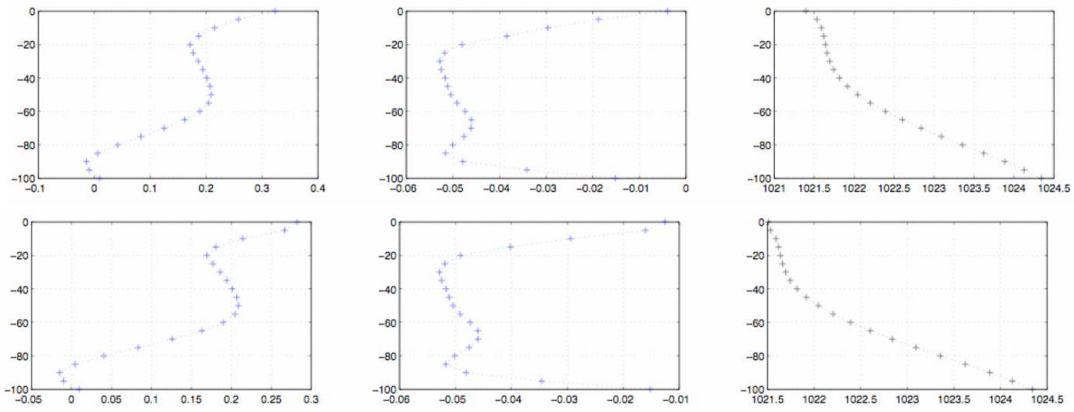
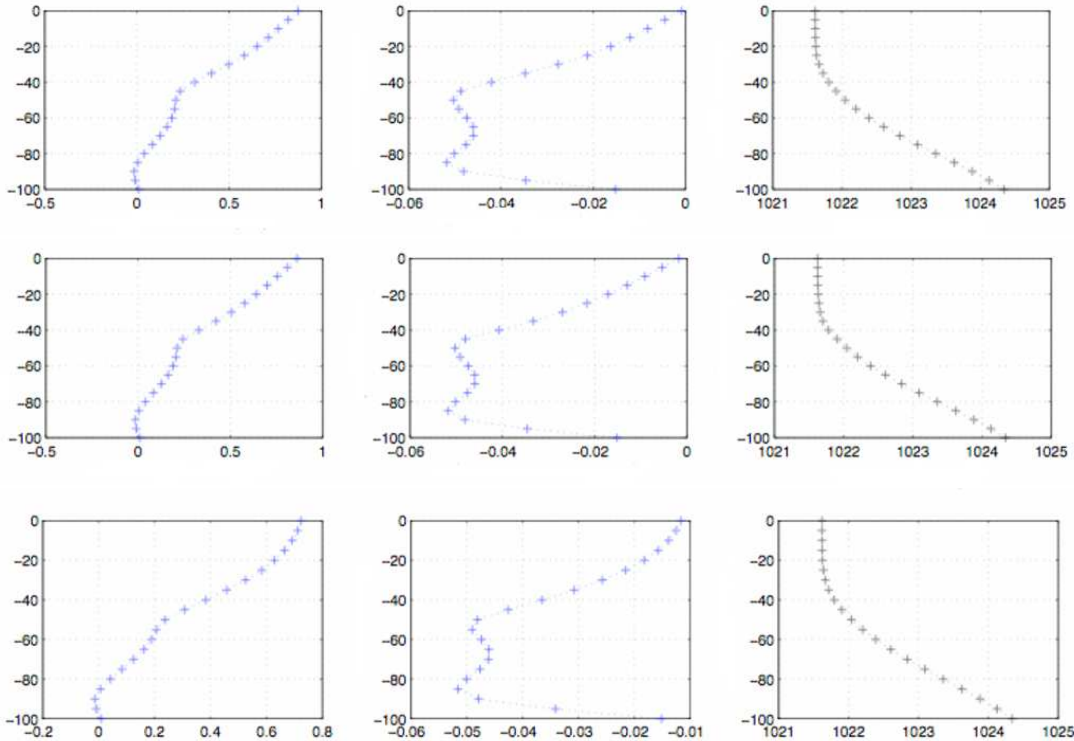


Figure 8 : Final zonal velocity, meridional velocity and density profile for respectively from top to below for R224, R213, R23 and R22 model.

On the velocity profile, we observe that the surface current values, for R224 model, are between R213 and R23 model's. The R22 model gives as results a weak surface current. The density profile show that R224, R213 and R23 reproduces the initial density profile in this form. For the surface value, R23 and R224 model gives same results. The surface density is slightly higher for R22 and R213 model. In addition, for these latter model, we have the same values of density surface. For all models, we have no mixed layer and we can not compare these models neither on the mixed layer depth nor on the thermocline's form.

Second Case : Strong wind at the surface



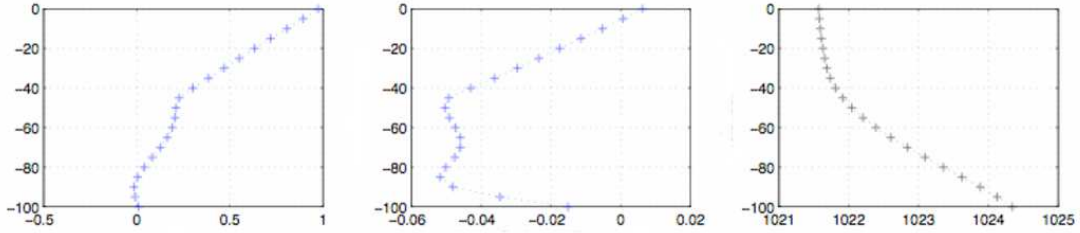


Figure 9 : Final zonal velocity, meridional velocity and density profile for respectively from top to below for R 224, R 213, R 23 and R 22 model.

The velocity profile show, for the intensity of the current surface, similar results for R 213 and R 224 model. The R 23 model simulate a weaker surface current and the R 22 model give a larger surface current. The density profile show a mixed layer of twenty meters deep for R 213, R 224, R 23 model with the same criterion that Peters and al [32]. The R 22 model does not produce a mixed layer. The thermocline simulated by R 224 and R 213 model has the same characteristic. All models gives similar results for the flow between 60–100 m because the surface fluxes are not enough large to affect the deep water.

Sensitivity to density gradient In this case, we study the day of 17/11/91. We have for this day a South-West wind at the surface with a zonal component of 11.7 m s^{-1} and a meridional component of 0.4 m s^{-1} . The value choose for the density flux is $-1e-6 \text{ kg m}^{-2} \text{ s}^{-1}$. The initial zonal velocity profile presents a eastward current whose maximum is located about 55 m. Then the zonal velocity decreases. The initial meridional velocity profile presents a southward current whose maximum is located about 20 m. The initial density profile presents an inversion of density gradient located about 30 m. We observe a mixed layer seventy meter deep according to the same density criteria that Peters et al [32]. However, this mixed layer is not homogeneous. The initial profiles are plotted on the figure 10.

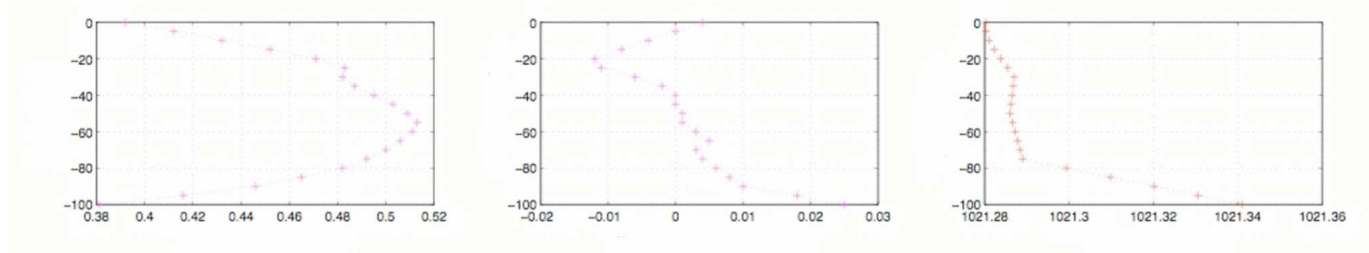


Figure 10 : The initial profile for zonal velocity, meridional velocity and density for the different depths.

We plot the initial richardson number on the figure 15.

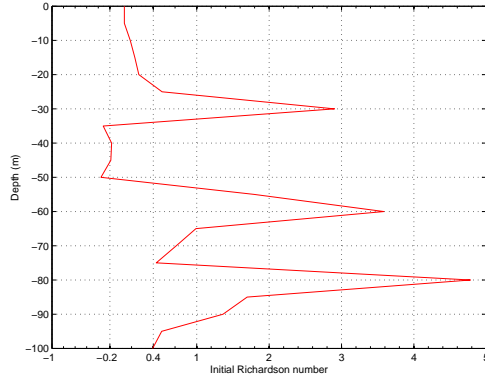


Figure 11 : The initial richardson number for the di erent depths.

On the previous gure, we observe that for depth of 35 m and 50 m , the richardson number is inferior to 0.2 and therefore, the di usivity of R213 m odel is negative. For a depth into [35; 50 m], we rem ark that the richardson number is inferior to 0.1 and hence the di usivity of R23 m odel is so negative. In addition, we note that for a depth of 40 m and 45 m , the richardson number is around to 0.2, value for which the di usivity of R213,R22,R224 m odel is in nite.

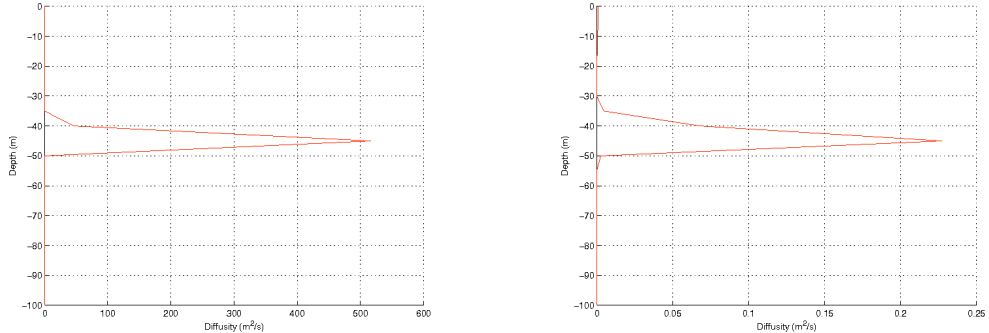


Figure 12 : Initialdi usivity for formulations R224 (left hand side) and R22 (right hand side).

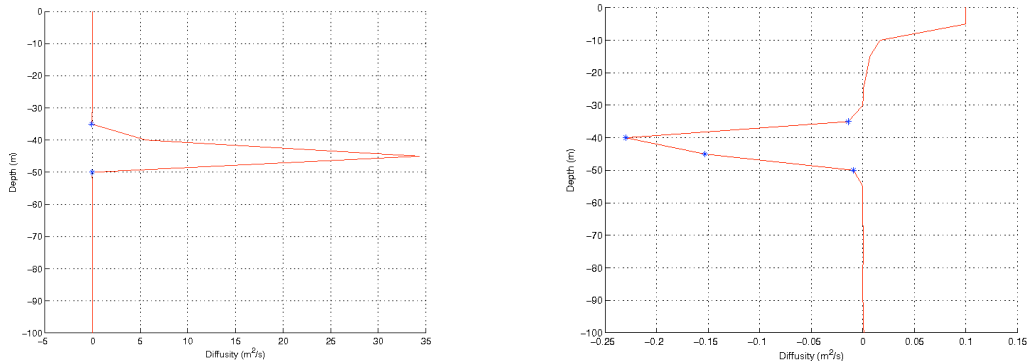


Figure 13 : Initialdi usivity for formulations R213 (left hand side) and R23 (right hand side).

On the richardson number's graph, we observe a value about 0.2 for a depth of 45 m. This value is singular for models R 224, R 22 and R 213 which is in agreement with the large value of the diffusivity for these models at this depth. On the figure 17, the negative value of diffusivity is marked by an asterisk. We note that the R 22 and R 224 models have not negative values. On the contrary, R 213 and R 23 models have negative values. The problem is that physically, it is not possible to have a negative diffusivity. The vertical eddy diffusivity was estimated notably by Obourn and Cox [29] with measurements of very small scale vertical structure. In our studied region, the diffusivity can vary between $1:10^2 \text{ cm}^2 \text{ s}^{-1}$ and $1:10^3 \text{ cm}^2 \text{ s}^{-1}$, but, in all case, this value is always positive. So, we can not use R 213 and R 23 models for this case.

We $\times T = 48 \text{ h}$ and we make the simulations with the initial conditions described above. We obtain the results on the figures 18 and 19.

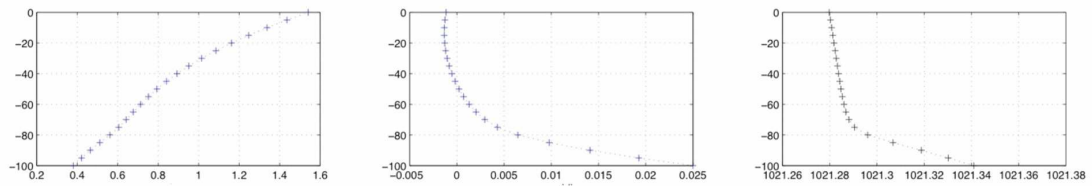


Figure 14 : R 224 : The profile for zonal velocity, meridional velocity and density for the different depths.

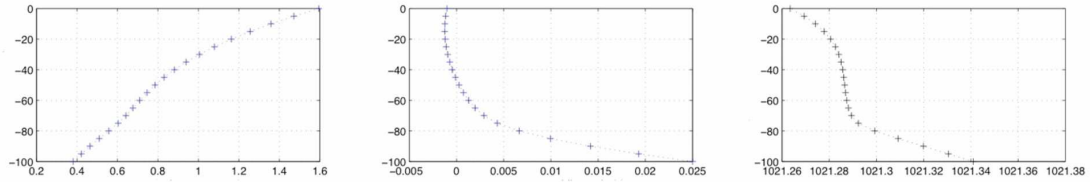


Figure 15 : R 22 : The profile for zonal velocity, meridional velocity and density for the different depths.

On the figure 15, we note no mixed layer. On the contrary, the R 224 model produce a homogeneous mixed layer to seventy meter deep with no density gradient inversion. The velocity profile show a larger surface current for the R 22 model. This fact is agree with the results of previous section. R 22 and R 224 model gives same results for the range [100; 60 m] because the surface fluxes not modify the deep water.

Summary on the realistic case The test on the sensitivity to the flow to the wind stress intensity show similar results to the linear case. For a shallow wind, we have no mixed layer whereas for a strong wind, we have a mixed layer. The comportment of all turbulence models, for the surface current intensity and for the mixed layer depth is the same as linear case. In contrary, the three model, R 224, R 213 and R 23, for the thermocline's form, gives different results in linear case and in realistic case. We observe, for the sensitivity on the density gradient, that, in statically instability situation, only R 224 model give good results.

4 Summary and Discussion

The linear case show, in first, the influence of wind stress intensity. In fact, with the linear initial density profile, with a strong wind, we product a mixed layer ten meter deep for a time equal to 48 h. The time evolution of initial velocity profile show our modelization is good because by applying a eastward wind and northward wind, we note the increasing to the surface current.

The long time case, based on the initial data from TAO array (McPhaden [24]), show that we tend on a linear equilibrium solution which is agree to the results of Bennis and al [1].

The different studied case allow to expose the advantages and drawbacks for each turbulence model. We remind that the comparison is based on three criterion : the mixed layer depth, the surface current intensity and the thermocline's form .

For the mixed layer depth, the R 213, R 23 and R 224 model gives same results. The R 22 model does not product a mixed layer. For the formation of the mixed layer, the three model show the same sensitivity to the wind stress intensity.

For the surface current intensity, for the case of strong case, we observe the same tendency. R 224 and R 213 model product a similar surface current with slightly higher values for R 224 model. R 23 model underestimate this current while the R 22 model overestimate it. For the shallow wind, we observe for the R 213 and R 224 model the same comparison that the strong wind case. In contrary, the R 22 model overestimate this current while the R 23 model underestimate. The simulation for a long time show that the surface current evolve as the strong wind case. Therefore, the comparison for shallow wind for R 23 and R 22 model is not representative. In the long time case, R 23 and R 22 model gives incorrect results in comparison with R 213 and R 224 model.

For the thermocline's form, the linear case, for strong wind case, show that the thermocline simulated by the R 224 model is sharpest that for the R 213 and R 23 model. R 22 model does not product a mixed layer and therefore we can not study the thermocline. For the realistic case, R 23, R 213 and R 224 model simulate a thermocline which has the same characteristic.

The 17/11/91 case show that only R 22 and R 224 model represent a physical realistic situation. In fact, the R 213 and R 23 model are a negative dissimilarity at the initial time that is not physically realistic. This problem comes from to the density gradient inversion around to 30 m . Hence, we can not use these model in this case. R 224 model product a homogeneous mixed layer without increase its depth.

Excepted for the long time case, all models gives similar results into [100; 60 m] because the surface fluxes does not affect the deep water for a time equal to 48 h. In the contrary, for a long time, these fluxes model the deep water and this is the reason which we have a different results for a time equal to 10000 h.

Finally, we conclude that the R 22 model is not good for the simulation of the mixed layer and the surface current. R 224 model has a same problem that the R 213 model, it overestimate the surface current. However, it give a better results than R 23 model on this point. For the linear case, the R 224 model is the better model for the thermocline simulation. In fact, an another problem of R 213 model is to simulate a too diffuse thermocline and R 224 gives a sharpest thermocline than R 23 and R 213 model. For the mixed layer depth the R 224 model gives same results that R 213, R 23 model. In addition, for the case where we are in statically instability, only R 224 model is physically valid and it gives a homogeneous mixed layer. R 224 have in general the same behavior that the Pacanowski and Philander model and we can use it for more situation.

References

- [1] A . C . Bennis, T . C . Rebollo, M . G . M armol, and R . Lewandowski, Stability of some turbulent vertical models for the ocean mixing boundary layer, *Applied Mathematical Letters*, To Appear (2007).
- [2] B . Blanke and P . Delecluse, Variability of the tropical atlantic ocean simulated by a general circulation model with two different mixed-layer physics, *J. Phys. Oceanography*, 23 (1993), pp. 1363{1388.
- [3] K . Brainerd and M . G regg, Surface mixed layer and mixing layer depths, *Deep Sea research*, 42 (1995), pp. 1521{1543.
- [4] J. W . Deardorff, G . W illis, and D . Lilly, Laboratory investigation of nonsteady penetrative convection, *J. Fluid. Mech.*, 35 (1969), pp. 7{31.
- [5] A . Defant, *Schichtung und zirkulation des atlantischen ozeans*, *W iss. Ergebni. Deutsch. Atlant. Exp. Meteor.*, 6 (1936), pp. 289{411.
- [6] E . Deleersnijder, Echelles de temps determinante, ou determinante par, les écoulements des fluides géophysiques, *Bul. Soc. Roy. Sci. Liege*, 67 (1998), pp. 43{68.
- [7] A . Garbett and T . R . Osborn, Small scale shear measurements during the ne and microstructure experiment, *J. Geophys. Res.*, 86 (1981), pp. 1929{1944.
- [8] P . R . Gent, The heat budget of the toga-coare domain in an ocean model, *J. Geophys. Res.*, 96 (1991), pp. 3323{3330.
- [9] H . Goosse, E . Deleersnijder, T . F ichefet, and M . H . England, Sensitivity of a global coupled ocean-sea ice model to the parametrization of vertical mixing, *J. Geophys. Res.*, 104 (1999), pp. 13681{13695.
- [10] M . C . G regg, Temperature and salinity microstructure in the pacific equatorial undercurrent, *J. Geophys. Res.*, 81 (1976), pp. 1180{1196.

[11] M . C . G regg and T . B . Sandford, Signature of mixing from the bermuda slope, the sargasso sea and the gulf stream , *J. Phys. Oceanogr.*, 10 (1980), pp. 105{127.

[12] D . Halpern, Y . Chao, C . Ma, and C . M echoso, Comparison of tropical pacific temperature and current simulations with two vertical mixing schemes embedded in ocean general circulation model and reference to observations, *J. Geophys. Res.*, 100 (1995), pp. 2515{2523.

[13] A . C . H irst and T . J . M . D ougall, Deep-water properties and surface buoyancy flux as simulated by a z-coordinate model including eddy-induced advection, *J. Phys. Oceanogr.*, 26 (1996), pp. 1320{1343.

[14] R . H . K ase, Modeling of the oceanic mixed-layer and effects of deep convection, 1998.

[15] E . Kraus and J . Turner, A one dimensional model of the seasonal thermocline, ii, the general theory and its consequences, *Tellus*, 19 (1967), pp. 99{105.

[16] W . G . Large, G . Danabasoglu, S . C . D oney, and J . C . M . Williams, Sensitivity to surface forcing and boundary layer mixing in a global ocean model : Annual mean climatology, *J. Phys. Oceanogr.*, 27 (1997), pp. 2418{2447.

[17] W . G . Large and P . R . Gent, Validation of vertical mixing in an equatorial ocean using large eddy simulations and observations, *J. Phys. Oceanogr.*, 29 (1999), pp. 449{464.

[18] W . G . Large, C . M . Williams, and S . C . D oney, Oceanic vertical mixing : a review and a model with a nonlocal boundary layer parameterization, *Rev. Geophys.*, 32 (1994), pp. 363{403.

[19] M . lesieur, *Turbulence in Fluids*, Kluwer, 1997.

[20] S . Levitus, *Climate atlas of the world ocean*, U . S . G ov . P rinting O ffice, Washington, 1982.

[21] R . Lewandowski, *Analyse mathématique et oceanographie*, Masson, 1997.

[22] X . Li, Y . Chao, J . M . Williams, and L . Fu, A comparison of two vertical mixing schemes in a pacific ocean general circulation model, *Journal of Climate*, 14 (2001), pp. 1377{1398.

[23] G . M adec, P . D ecleuse, M . Imbard, and C . Levy, *OPA version 8.0. ocean general circulation model, reference manual*, 1997. Technical report.

[24] M . M cPhaden, The tropical atmosphere ocean (tao) array is completed, *Bull. Am . Mетеoro. Soc.*, 76 (1995), pp. 739{741.

[25] G . Mellor and T . Yamada, Development of a turbulence closure model for geophysical fluid problems, *Reviews of Geophysics and Space Physics*, 20 (1982), pp. 851{875.

[26] C. B. Montegut, G. M. Madec, A. S. Fischer, A. Lazar, and D. Iudicone, Mixed layer depth over the global ocean : An examination of profile data and a profile-based climatology, *Journal of Geophysical Research*, 109 (2004), p. C12003.

[27] G. M. Montrey and S. Levitus, Seasonal Variability of Mixed Layer Depth for the World Ocean, *NOAA Atlas NESDIS 14, National Oceanic and Atmospheric Administration*, Silver Spring, 1997.

[28] P. P. Niiler and Coauthors, Comparison of toga tropical ocean model simulations with the woce/toga surface velocity programme drifter data set., *World Climate Research Programme Report WCRP-1995*, (1995), p. 156pp.

[29] T. O. Sborn and C. Cox, Oceanic neststructure, *Geophys. Fluid Dyn.*, 3 (1972), pp. 321-345.

[30] R. C. Pacanowski and S. G. H. Philander, Parameterization of vertical mixing in numerical models of the tropical oceans, *J. Phys. Oceanogr.*, 11 (1981), pp. 1443-1451.

[31] H. Peters, M. C. G. Regg, and J. M. Toole, On the parameterization of equatorial turbulence, *Journal of Geophysical Research*, 93 (1988), pp. 1199-1211.

[32] —, Meridional variability of turbulence through the equatorial undercurrent, *Journal of Geophysical Research*, 94 (1989), pp. 18,003-18,009.

[33] S. G. H. Philander, *La Niña, and the Southern Oscillation*, Academic Press, 1990.

[34] C. Rossby and R. M. Montgomery, The layer of frictional influence in wind and ocean current, *Pap. Phys. Oceanogr. Met.*, 3 (1935), pp. 1-101.

[35] T. Shay and M. G. Regg, Convectively driven turbulent mixing in the upper ocean, *J. Phys. Oceanography*, 16 (1986), pp. 1777-1798.

[36] N. R. Smith and G. D. Hess, A comparison of vertical eddy mixing parameterizations for equatorial ocean models, *J. Phys. Oceanography*, (1993), pp. 1823-1830.

[37] E. G. Tabak and F. A. Tal, Turbulent mixing of stratified flows, *Cubo Mat. Educ.*, 6 (2004).

[38] J. Vialard and P. D. delecluse, An ocean study for the toga decade. part i: Role of salinity in the physics of the western pacific fresh pool, *J. Phys. Oceanogr.*, 28 (1998), pp. 1071-1088.